Thermal blooming measurement of specific heat and thermal conductivity in isotropic *p*-methoxy benzylidene *p*-butylanyline (MBBA) near clearing

G. Koren
IBM Zurich Research Laboratory, 8803 Rüschlikon, Switzerland
(Received 23 June 1975)

Using the thermal-lens effect, the specific heat C_p and the thermal conductivity Λ have been measured simultaneously in the isotropic phase of the liquid crystal MBBA (*p*-methoxy benzylidene *p*-butylanyline) near its isotropic-to-nematic transition. Accurate analysis of the lens dynamical behavior yields both transport coefficients provided the change of the refractive index with temperature, dn/dT, is known. A precise measurement of $n(T)$ was carried out separately. The best fits yield the critical exponents 0.52 and 0.65 for C_p and Λ, respectively, with a critical temperature T_c equal to $T_p - 0.21 \pm 0.01$ °C, where T_p is the clearing temperature. The present measurements give the first conclusive results on the critical behavior of C_p in the isotropic phase of a liquid crystal.

INTRODUCTION

Calorimetric methods and thermal flow techniques have long been used to measure transport coefficients accurately. Near phase transitions, however, these techniques are time consuming and hard to perform. They are also intrinsically limited in the possibility of sufficiently approaching the critical temperature. Measurements of C_p and Λ in *p*-methoxy benzylidene *p*-butylanyline have already been reported.[1,2] Using a calorimetric technique, C_p was measured over a wide temperature range but in wide temperature steps. The thermal-conductivity measurement[2] was made with thermal gradients of approximately 1–2 °C. Thus neither measurement is fine enough near the isotropic-to-nematic transition to allow for quantitative conclusions to be drawn about the critical behavior. Photon-beating spectroscopy of scattered light has been used to measure the thermal diffusivity coefficient $D = \Lambda/\rho C_p$, but this method does not allow for a determination of each parameter separately.

A very simple and accurate optical means of obtaining both C_p and Λ in transparent materials is to measure the thermal defocusing (also known as thermal blooming) of a laser beam in the sample.[3–5] This method perturbs the sample to a negligible extent and its principles are as follows: A small fraction of the light is absorbed along the laser trace, causing local heating. This produces a cylindrical thermal gradient in the sample, which yields a divergent or convergent lens, depending on whether the change in the refractive index with temperature, dn/dT, is negative or positive, respectively. From the first observation of the thermal-defocusing effect[3] it was clear that this method could be used to measure D, Λ, and C_p, or if some of these are already known, alternatively to measure dn/dT and small absorbancies.[4] A few years ago, Calmettes and Laj[5] suggested using this method to determine D and Λ simultaneously near the phase transitions of transparent liquids and solids; a simple setup avoiding previous drawbacks is reported in their work. They were especially interested in measurements near the critical point of binary-liquid mixtures, but apparently they could not achieve sufficient accuracy. No new measurements using this method have been published since. Recently, Giglio and Vendramini[6,7] have successfully measured the diffusion constant and the thermal-diffusion ratio in a binary mixture near the critical temperature, using thermal blooming and the classical Sorret effect, but they did not use the method to measure C_p and Λ.

The purposes of this paper are (i) to establish the quantitative use of thermal blooming for the simultaneous measurement of C_p and Λ and (ii) to give a representative, accurate measurement in isotropic MBBA near its phase transition. The possibility of obtaining reliable results quickly and in a very simple way is shown, and the advantages and limits of applying the method are discussed. A separate interferometric measurement of the refractive index of the isotropic MBBA as a function of temperature, using a folded Jamin interferometer,[8,9] is described, and the values of Λ and C_p are calculated using this and the thermal-lens data. It was necessary to remeasure $n(T)$ since the data available in the literature were insufficient.[10] Finally, the results for MBBA are analyzed on the basis of existing theories. The critical exponents of C_p and Λ are found and a comparison with other measurements is given.

EXPERIMENTAL

The experimental system used to measure the thermal-lens effect is described schematically in

Fig. 1. The main differences from previous work[5] are the use of a dielectric coated mirror and of a thick glass slide instead of metallic mirrors, and the direct use of a computer terminal. This terminal processed the data during measurement not only for convenience but also in order to check fluctuations in the measured parameters and repeat measurements if necessary within the same run. The thick glass slide was used as mirror and attenuator for the laser beam. The measurements are performed as follows: The shutter opens rapidly, and the fast photodiode triggers the scanning of the multichannel memory, which collects the signal from the photomultiplier PM. The photomultiplier measures the light passing through the pinhole, whose diameter is smaller than the beam diameter in the absence of the sample. A typical experimental result is shown in Fig. 2, where the continuous curve is drawn through the measured points. The fits will be discussed later. A test measurement without sample shows that the beam suffers no defocusing up to laser intensities of approximately 1 W. Thus the signal is due only to the sample. The measurements were performed with a vertical beam, as suggested in Ref. 5, in order to preserve cylindrical symmetry.

The MBBA liquid crystal used is the best quality available from Kodak. It almost entirely filled a rectangular glass cuvette closed by a Teflon stopper. The optical length was 1 cm. The cuvette was mounted in a large brass block which was thermally stabilized to within ± 0.01 ° C. The color of the material is faintly yellow. Its dn/dT and absorption of the argon-ion laser's green and blue lines are sufficient to produce easily measurable thermal lenses for laser intensities of approximately 50 mW (see Fig. 2).

The familiar problem of deterioration of MBBA with time was observed.[10] This is indicated by the increase of the absorption coefficient α and the reduction in the clearing temperature T_p. In the course of nearly two months α varied by a factor of ~2 and T_p changed from approximately 45.5 to ~42 ° C. T_p was measured frequently and the results are presented as a function of $T - T_p$. Calibration for the variations of α is not necessary since the final measurement was carried out in one day and with $T_p \approx 42$ ° C. A few measurements, however, were performed with the fresher material, and no significant difference in the behavior of the transport coefficients as a function of $T - T_p$ was observed.

The measurement of the refractive index as a function of temperature $n(T)$ was performed with a modified Jamin interferometer.[8,9] This interferometer is composed of a thick plate of glass and a rectangular prism, mounted in such a way that the large face of the prism and the face of the plate are at an angle of 45° to each other. A collimated beam is incident on the plate at an angle of about 45°; the light is reflected to the prism from both faces of the plate, reflected back to the plate by the prism, and reflected again by the plate, parallel to the source beam, producing an interference pattern. The sample is placed in the beam path between the prism and the plate, and the interference pattern changes with the change in optical path length. In this way, the

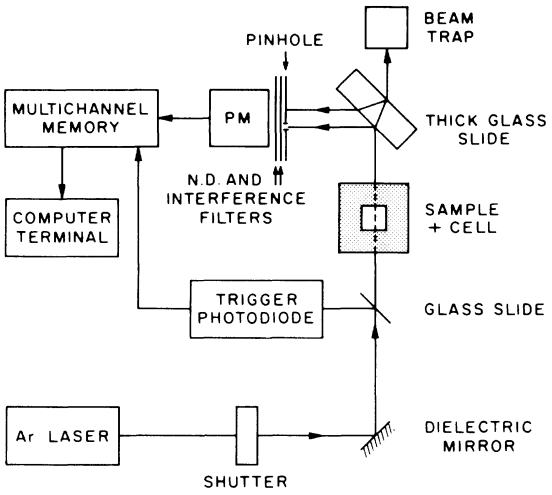

FIG. 1. Schematic diagram of the experimental system.

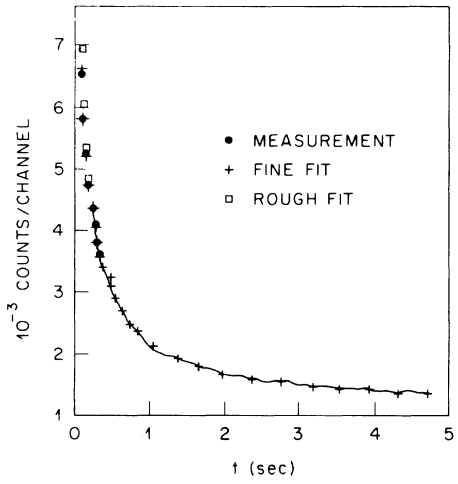

FIG. 2. Typical thermal-lens measurement. The dots and the continuous line are the experimental values (120 points). The squares are calculated from the rough fit of Eq. (14) and the crosses are calculated from the finer fit of Eq. (15). Owing to lack of drawing space, not all crosses are shown, and in cases where squares and crosses coincide, only the crosses are shown.

fringe pattern produced by 1 cm of MBBA was measured as a function of temperature. The change of path length due to the cuvette windows and to its thermal expansion is negligible, so that one obtains immediately $\Delta n(T) = n(T) - n(T_{cn})$, where T_{cn} is defined below.

Since the refractive index was measured with a horizontal beam, one can reach a lower temperature in this measurement than in the thermal-lens (TL) measurement performed with a vertical beam. The difference is due to gravity. The TL measurement is terminated immediately at clearing, because drops of nematic material distort the lens. In addition, a rise of the tail in Fig. 2 is observed, owing to laser heating which clears the nematic drops. In the refractive-index measurement, the drops of nematic material sink to the bottom of the cuvette (because of the higher density of the nematic phase).[11-13] The intensity of the fringes decreases, due to scattering by the nematic drops, and the measurement is terminated at a temperature T_{cn} where fringes disappear. At this temperature a large fraction of the material is nematic. One should stress that this is possible only because a stable two-phase region exists in MBBA.[11-13] It can be reduced by using purer material.[13] The clearing point is identified as the point where the fringe contrast decreases abruptly owing to nematic drops scattering. It was found from a number of measurements that the difference $T_p - T_{cn}$ is ~0.18 °C in our case.

The results of Δn as a function of temperature for the HeNe laser wavelength $\lambda = 6328$ Å are shown by the dots in Fig. 3. The experimental values were taken from the fringes of the best measurement, and the results are reproducible, as was found in five additional measurements

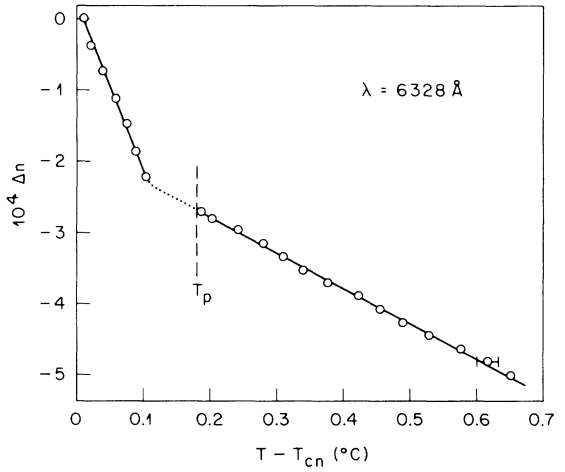

FIG. 3. Change in the refractive index as a function of temperature.

made while sweeping the temperature slowly up and down through the transition. Measurements of $\Delta n(T)$ in the temperature region $T_{cn} + 0.7$ °C $\lesssim T \lesssim 60$ °C were also performed; the spacing of the fringes in this region is constant as a function of temperature, and therefore is not shown in Fig. 3. Note that the dispersion in dn/dT is very small;[10] hence our results at $\lambda = 6328$ Å were deliberately used also for analyzing TL data taken with $\lambda = 4880$ Å. Examining Fig. 3, one sees that $\Delta n(T)$ varies rapidly only near T_{cn}, where the nematic and isotropic phases coexist. In the isotropic region above clearing, $\Delta n(T)$ is almost linear as a function of temperature, and therefore dn/dT is to a very good approximation a negative constant. The Lorentz-Lorenz relation shows this to be in agreement with the density measurements[11-13] well above clearing.

ANALYSIS OF THE TL MEASUREMENT

To analyze the TL measurement, the theoretical shape of the curve shown in Fig. 2 is needed. The detailed calculation of Ref. 5 is briefly repeated here in a modified form which includes scattering. Note that scattering is important especially near phase transitions. Let us assume that a Gaussian beam of radius ω at the sample and total power P_0 is switched on at time $t = 0$, and is propagating along the x direction in the almost transparent sample. Solving the heat-diffusion equation, one obtains the time-dependent temperature distribution as a function of the radial distance from the axis r in terms of exponential integrals:[3,5]

$$\delta T(r, x, t) = \frac{\alpha P_0}{4\pi\Lambda}\left[\mathrm{Ei}\left(-\frac{2r^2}{\omega^2}\right) - \mathrm{Ei}\left(-\frac{2r^2}{\omega^2 + 8Dt}\right)\right] e^{-\beta x}\ ; \quad (1)$$

α is the absorption coefficient, β is the total loss coefficient (absorption plus scattering), and D is the thermal-diffusion coefficient

$$D = \Lambda/\rho C_p\ . \quad (2)$$

The temperature distribution of Eq. (1) causes a refractive-index distribution given by

$$\delta n(r, x, t) = \frac{dn}{dT}\,\delta T(r, x, t)\ . \quad (3)$$

For $\beta l \ll 1$, where l is the length of the sample, using geometrical optics, one finds in first-order approximation that the rays follow a circular path in the sample. Their radius of curvature R is given by[14]

$$\frac{1}{R(r,t)} \cong \frac{1}{n}\frac{\partial}{\partial r}\,\delta n(r,t) = -\frac{1}{n}\frac{dn}{dT}\frac{\alpha P_0 r}{\pi\omega^2\Lambda}\,\frac{t}{t + t_c}\ , \quad (4)$$

where Eqs. (1) and (3) were used to obtain the right-hand side of Eq. (4) and where

$$t_c \equiv \omega^2/8D . \tag{5}$$

When βl is not negligible, the radius of curvature is not only time dependent but also a function of x. Thus for paraxial rays one obtains

$$1/R(r, x, t) = [1/R(r, t)]\, e^{-\beta x} , \tag{6}$$

where the x component of the gradient of $\delta n(r, x, t)$ is neglected and $R(r, t)$ is defined in Eq. (4). Using the definition of the radius of curvature and neglecting its x component, one can calculate the radial component, which is given by

$$\frac{1}{R(x, r, t)} = \left[1 + \left(\frac{dr}{dx}\right)^2\right]^{-2} \frac{d^2r}{dx^2} . \tag{7}$$

Since $dr/dx \ll 1$ (i.e., we are dealing with small deviation angles), Eq. (7) is easily solved for the exit angle before refraction. The result is

$$\left(\frac{dr}{dx}\right)_{x=l} = \frac{1}{R(r, t)} \frac{1 - e^{-\beta l}}{\beta} , \tag{8}$$

where the boundary condition $(dr/dx)_{x=0} = 0$ is assumed. Assuming further that the distance L between the sample and the pinhole is much longer than the cell length l, the radius of the beam at the pinhole is given by

$$\rho(r, t) = r + nL\left(\frac{dr}{dx}\right)_{x=l} , \tag{9}$$

where r is the radius of the original beam. Substituting Eqs. (4) and (8) in Eq. (9), one can calculate the maximal radius $r_{\max}(t)$ of the source rays for which there is a contribution to the photocurrent through the pinhole of radius ρ_0. This gives

$$r_{\max}(t) = \rho_0 \left(1 - \frac{\alpha\, lL\, P_{\text{eff}}}{\pi \omega^2 \Lambda} \frac{dn}{dT} \frac{t}{t + t_c}\right)^{-1} , \tag{10}$$

where

$$P_{\text{eff}} \equiv P_0 (1 - e^{-\beta l})/\beta l . \tag{11}$$

Note that P_{eff} is also equal to the average of the intensity along the beam. Equation (10) immediately yields the time-dependent light intensity which contributes to the photocurrent:

$$P(t) = P_{\text{tr}} \frac{2 r_{\max}^2(t)}{\omega^2} = K^2 \left(\frac{t + t_c}{zt + t_c}\right)^2 , \tag{12}$$

where

$$z \equiv 1 - \frac{\alpha\, lL\, P_{\text{eff}}}{\pi \omega^2 \Lambda} \frac{dn}{dT}, \qquad K^2 \equiv \frac{2\rho_0^2 P_{\text{tr}}}{\omega^2} , \tag{13}$$

and where P_{tr} is the transmitted intensity. Neglecting initial beam divergence over the sample, and with the assumption that $l \ll L$, Eqs. (12) and (13) are similar to the results given by Calmettes and Laj,[5] after correction for a number of misprints.

It was found experimentally that the curve in Fig. 2 follows Eq. (12) accurately. In order to check the validity of the above linear theory, the parameters z and t_c were measured as a function of laser intensity at constant temperature ($T \approx 45$ °C). The intensity of the laser was changed by varying the excitation current rather than by using neutral-density glass filters, whose thermal focusing changes ω significantly. The results of this measurement for z are shown in Fig. 4. One sees that z is equal to 1 when the intensity is zero, in agreement with Eq. (13), and that z varies linearly at low intensities. A similar behavior was also found in a binary mixture in Ref. 6. The parameter t_c was found to be almost constant in this measurement, excluding small variations in ω for different laser excitation currents. Hence for sufficiently low laser intensities Eq. (12) is adequate, and was used to fit the experimental data by least squares.

In their work, Calmettes and Laj used a nonlinear statistical refining method developed by Tournarie,[15] but did not elaborate on the details of their program, which may be crucial in obtaining reliable results. The fitting procedure presently used is the following: As the first step, it is possible to use a usual linear fit procedure on

$$(z/c)\, t \sqrt{I(t)} + (t_c/c)\sqrt{I(t)} - t_c - t = 0 , \tag{14}$$

which is equivalent to Eq. (12). Here $I(t)$ is the measured photocurrent and c is a constant proportional to K, which is defined in Eqs. (12) and

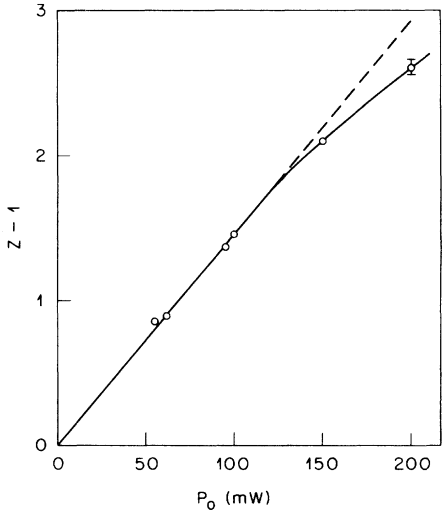

FIG. 4. Parameter $z - 1$ as a function of laser intensity.

(13). Equation (14) is treated as a system of n equations (number of measured points) with three unknowns, z/c, t_c/c, and t_c. The results of such a fit give approximate values for c, z, and t_c and are shown by the squares in Fig. 2. It is clear, however, that one has to fit to the experimental results a formula of the form of the right-hand side of Eq. (12) and not Eq. (14). Taking into account the statistical error in the photocurrent, which is proportional to $\sqrt{I}$, one finds that the fits have to be made by minimizing the standard rms error of $\sqrt{I(t)}$ rather than that of $I(t)$. Indeed, in the least-squares fit procedure, the quantity to be minimized is $\sum_i (I_i - f_i)^2/(\sqrt{I_i})^2$, where f_i are the calculated-values function of the parameters. However, since the approximate values of the parameters c_0, z_0, and t_{c0} are available from the fit of Eq. (14), an iterative procedure is used, in which one starts with fairly good values for f_i, i.e., $f_i \approx I_i$ (see the squares in Fig. 2). The minimization of the above expression is then equivalent to that of $4\sum_i (\sqrt{I_i} - \sqrt{f_i})^2$; hence one can work with $\sqrt{I}$ as we have done. Thus using c_0, z_0, and t_{c0} as initial values in a power series expansion of c, z, t_c in an Eq. (12) type for the photocurrent, and keeping only first-order terms, one obtains a linearized equation

$$\sqrt{I} + \Delta\sqrt{I} = (c_0 + \Delta c)\frac{t + t_{c0}}{z_0 t + t_{c0}} + \frac{c_0 t(z_0 - 1)}{(z_0 t + t_{c0})^2}\Delta t_c - \frac{c_0(t + t_{c0})t}{(z_0 t + t_{c0})^2}\Delta z . \quad (15)$$

Equation (15) is easily fitted using a linear fit procedure. The new values for the three parameters are then reused in a repeated iteration process, and the procedure is stopped when a good convergence is achieved (i.e., when an improvement of less than 10^{-6} in the rms error is found). Usually two to four iterations are sufficient to obtain good convergence. An example of such a fit is given in Fig. 2 by the crosses. The improvement in the fit in comparison with the fit of Eq. (14) by using Eq. (15) is evident.

It was found experimentally that in order to obtain good convergence of the fit and to minimize the standard rms deviation, one should measure for a time duration t greater than $\sim 4t_c$ but smaller than $\sim 10t_c$. These limits give a good balance between the effects of C_p and Λ in the experimental response; the beginning of the response is entirely controlled by C_p and the tail by Λ. The lower limit allows the lens to form, while the upper limit is necessary in order to limit the weight of the points in the tail and reduce the effect of fluctuations in the tail that result from variations in the laser intensity. In good measurements the calculated values of t_c and z are almost independent of the termination point of the experimental curve between $\sim 4t_c$ and $\sim 8t_c$, and the standard rms deviation has a flat minimum in this region. In cases where this minimum is not flat, the parameters are chosen to be those with the minimum standard rms error.

The accuracy of the fits was further tested by measuring the absolute value of the thermal diffusivity D at room temperature in methanol. This was done by measuring both ω^2 directly by a set of calibrated pinholes and t_c from the fits. The very pure methanol used was faintly colored with iodine in order to increase accuracy. The optical path length was 1 cm, the laser intensity 50 mW, and $\lambda = 4880$ Å. The result, an average of six measurements, is $D = 0.98 \pm 0.03 \times 10^{-3}$ cm^2 sec^{-1}, which is in excellent agreement with the value found in handbooks, $D = 0.980 \times 10^{-3}$ cm^2 sec^{-1}. The accuracy of the measurement can still be improved by using a better-stabilized laser and averaging over a larger number of measurements.

RESULTS AND DISCUSSION

Following the above analysis, the experimental results for z and t_c are shown in Fig. 5. Each point is an average of at least five measurements. The laser intensity was 50 mW at $\lambda = 4880$ Å. At this intensity the beam heats the sample to less than 10^{-2} °C. ω^2 was measured by a set of calibrated pinholes and found to be 0.71 mm^2. (The pinhole used in the TL measurement was of diameter 0.5 mm.) The temperature-dependent transmission of the beam was measured with the same experimental setup but without pinhole. In

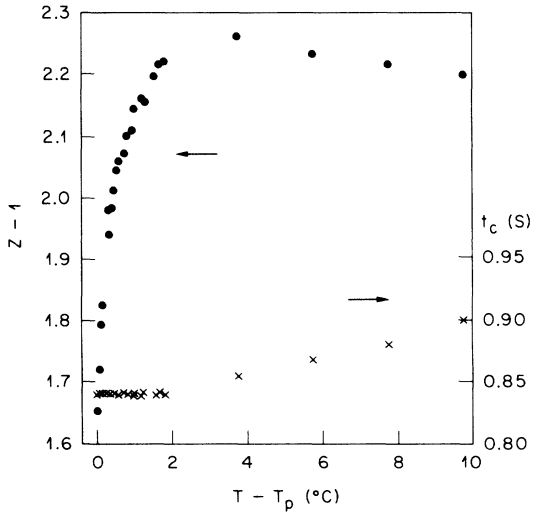

FIG. 5. Experimental $z-1$ and t_c as a function of temperature.

addition, the transmission without sample was also measured. From these, P_{eff}, which is defined in Eq. (11), was calculated (after correction for window reflection). The results for $z-1$ shown in Fig. 5 are calibrated with respect to P_{eff}. Note that the differences between the values of $z-1$ for $T-T_p \approx 2$ °C in Fig. 5, and for $T \approx 45$ °C and $P_0 = 50$ mW in Fig. 4, are due to different absorption coefficients of these samples. Since dn/dT is constant above T_p as seen from Fig. 3, the temperature-dependent behavior of Λ and C_p is easily calculated using Eqs. (2), (5), and (13). The absorption coefficient α of the MBBA being unknown, $C_p(T)$ was thus calibrated against the value measured at ~1.8 °C above T_p by Mayer *et al.*[1] (121 cal mol^{-1} deg^{-1}.) For this temperature, we find $D = 1.055\times10^{-3}$ cm^2 sec^{-1}, which also yields the calibration for $\Lambda(T)$ by using Eq. (2). (Λ at 1.8 °C above T_p is 4.9×10^{-4} cal cm^{-1} sec^{-1} deg^{-1}.) The results are shown in the insets of Figs. 6 and 7 by the dots. Comparing the C_p measured here with the data of Ref. 1, a fairly good agreement is found near the transition as well as in the tail. However, the published information does not allow a comparison in full detail. A comparison with the data of Ref. 2 is not possible, since the temperature difference applied in that measurement is between 1 and 2 °C, which smears all fine details near the transition. Furthermore, the cell used in Ref. 2 was thin. Hence surface effects plus strong convective instabilities in the high-temperature gradient used[16] prevent a comparison of Λ.

C_p and Λ were fitted by formulas of the form

$$A + B(T-T_c) + C(T-T_c)^{-G}, \tag{16}$$

where A, B, and C are constants found from a fit to the experimental data, treating T_c and G as parameters which are scanned until the best fit which minimizes the rms error is found. The noncritical or background part of Eq. (16) (C_{p0} and Λ_0) includes a linear temperature-dependent term to account for the increase in C_p and Λ at high temperature (see insets in Figs. 6 and 7).

Because a two-phase region coexists in our sample, one may ask what is the significance of an analysis which assumes a unique T_p and a unique T_c. A possible justification of this assumption is as follows: Let us suppose that the distribution of phase-transition temperatures results from depression of the transition by impurities (42 °C is a very low phase-transition temperature for MBBA) which are more soluble in the isotropic than in the nematic phase; they are thus concentrated in the remaining isotropic phase as droplets of nematic form, producing a further depression and the resulting width of the transition region. If this is so, one may argue that the impurities are uniformly distributed as long as the entire sample is isotropic, and therefore there is a unique phase-transition temperature which is equal to T_p.

The results of the fits are shown by the solid lines in Figs. 6 and 7. The numerical expressions obtained are

$$C_p = 96.65 + 2.6(T-T_p-0.20) + 28.38(T-T_p-0.2)^{-0.52}, \tag{17}$$

$$\Lambda = [4.268 + 0.050(T-T_p-0.22) + 0.863(T-T_p-0.22)^{-0.65}]\times10^{-4}, \tag{18}$$

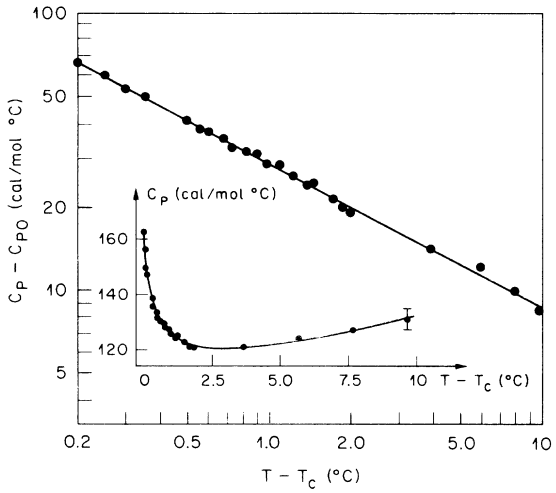

FIG. 6. C_p as a function of temperature. Dots: experimental points; lines: theoretical fit given by Eq. (17).

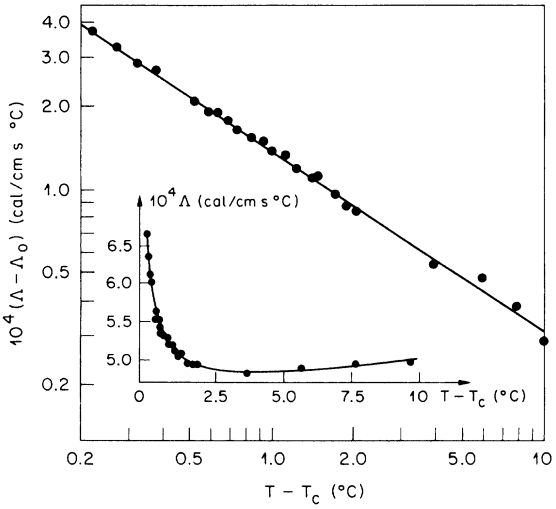

FIG. 7. Λ as a function of temperature. Dots: experimental points; lines: theoretical fit given by Eq. (18).

where the units of C_p are cal mol^{-1} deg^{-1} and those of Λ are cal cm^{-1} sec^{-1} deg^{-1}. One observes that the critical temperatures are the same within the experimental error for both C_p and Λ, ($T_c = T_p - 0.21 \pm 0.01$ °C), as they should be. This reflects the quality of the fits as T_c was optimized independently for both the C_p and the Λ data. The small rise of t_c in the higher-temperature region gives to C_p a bigger linear term than that of Λ, and as a result of this a slightly smaller exponent.

In the fitting procedure, the minimum of the rms deviation as a function of T_c and G is very flat. In the present experiments, the statistical accuracy in C_p and Λ is approximately $\pm 3\%$. If one allows for an increase of 3% in the rms error on both sides of its minimum as a function of T_c, and for the best G, one obtains for C_p

$$G = 0.52^{+0.21}_{-0.16}, \qquad T_c = T_p - 0.20^{-0.07}_{+0.05}\ ^\circ\mathrm{C},$$

and for Λ

$$G = 0.65^{+0.25}_{-0.16}, \qquad T_c = T_p - 0.22^{-0.08}_{+0.05}\ ^\circ\mathrm{C}.$$

The above limits represent the highly improbable but still possible curves that one can draw through the ends of the error bars in the data.

Several tests were performed to examine the quality of the fits. Omitting the first measured point changes all the parameters by less than 0.1%. This suggests that the transition temperature was sufficiently approached. Omitting the first four points (i.e., excluding a region of 0.3 °C from T_p) causes a severe deterioration of the fits; the exponents exceed 1 and $T_p - T_c$ is greater than 1–2 °C. A different test was made by fitting the experimental data only in the region close to the transition ($0 < T - T_p \leq 1.8$ °C). This yields a negative linear term for Λ [i.e., $B < 0$ in Eq. (16)] which has no physical significance. Thus taking a constant C_{p0} and Λ_0 in Eq. (16) one finds the exponent equal to 0.69 and $T_p - T_c = 0.21$ °C for both C_p and Λ, in agreement with Eq. (2) for constant D. Comparing these results with those of Eqs. (17) and (18), one sees that $T_p - T_c$ remains almost the same, as does the exponent of Λ, while that of C_p increases significantly. The overestimation of the exponent of C_p is due to the omission of the linear term in the fits. In short, we demonstrated that the transition temperature was sufficiently approached in the measurements, and that enough points were taken in the tail to obtain the correct linear term. In addition, a measurement in a higher-temperature region was performed. Fits including this region yield a deterioration of the rms error, presumably because a linear term alone in Eq. (16) is no longer sufficient to describe the behavior correctly. It seems that the temperature region chosen here ($0 < T - T_p \lesssim 10$ °C) is ideal for the quality and reliability of the fits.

Taking into account short-range order above clearing, it can be shown that the volume expansion coefficient $\beta(T)$, the correlation length $\xi(T)$, and $C_p(T)$ have the same exponents.[11,17] Local mean-field theory leads to an exponent ν of $\xi(T)$ equal to 0.5. The mean-field exponent of β and C_p is thus also 0.5.

Comparing the exponent G of $\beta(T)$[11,13] with the exponent of C_p obtained here (0.52), a good agreement with the results of Gulari and Chu[13] is found ($G = 0.54$). The value of G found by Press and Arrott[11] is 0.21, which disagrees with our results and with those of Ref. 13. However, $T_p - T_c$ found in Ref. 11 is approximately 0.3 °C, while $T_p \approx T_c$ was found in Ref. 13. Thus one should be careful in drawing conclusions from this comparison. Apparently the differences between the results of Ref. 11 and Ref. 13 depend not only on the accuracy of the measurements but also on the temperature range used for the fits and on the inclusion of points sufficiently close to the transition.

A measurement of C_p in the liquid-crystal *para*-azoxyanisole (PAA) was reported by Arnold.[18] His results were fitted within the framework of the mean-field continuum fluctuation theory of de Gennes and substantial agreement was found.[17] However, only two measured points are given in the region of 1 °C above clearing. Thus the fits are very sensitive to the omission of the first point. In addition, no attempt was made to find the exponent α of C_p from the measurement, but a value of $\alpha = 0.5$ was assumed *a priori*.[17] From the best fit of Arnold's data with Eq. (16) here one obtains the exponent $\alpha = 0.83$ and $T_p - T_c = 0.37$ °C. Without the first measured point, the results are $\alpha \gtrsim 10$ and $T_p - T_c \gtrsim 10$ °C. This emphasizes the extremely important role of the points near T_p. It also shows that if one had more points in the region of 1 °C above the transition, different values would probably be obtained. Imposing a value of $G = 0.5$ in the fit of Arnold's data yields an rms error higher by approximately 2.5% than the minimum, with $T_p - T_c = 0.23$ °C. Thus one cannot deduce conclusively the exponent of C_p from that measurement. Recently a measurement of C_p in MBBA over a wide temperature range has been reported.[19] In this measurement, the first measured point in the isotropic phase is taken at ~0.6 °C above clearing. Again no reliable conclusion can be drawn from these data.

Light-scattering measurements of the correlation length ξ in isotropic MBBA near the phase transition were reported previously.[20,21] These measurements are extremely delicate, and while no temperature dependence for ξ was found in Ref. 20, a temperature dependence with $\nu = 0.5$ was found in Ref. 21. The latter result, combined

with the prediction that C_p and ξ should have the same exponent, yields a good agreement with the present data. However, one should note that the fits in Ref. 21 assume $\nu = 0.5$ *a priori*. The scanning of ν in these fits might yield different results. Nevertheless, using the light-scattering value $\nu = 0.5$ and our value $\alpha = 0.52$ in the critical exponents relation $d\nu + \alpha \geq 2$ with the dimensionality $d = 3$, one finds that this relation holds almost as an equality, and this seems to support the reliability of both measured exponents.

An important result obtained here is that the mean-field fluctuation-theory predictions are fulfilled very close to the clearing temperature, and not only far away from it, as found in previous light-scattering and magnetic-birefringence measurements.[22] It is possible that the observed deviations in the exponents near clearing[22] are due to a measurement in the two-phase region, or alternatively that in the present results the critical temperature was not sufficiently approached, because of the two-phase region, to enable observation of these deviations.

CONCLUSIONS

The quantitative TL method has been established here as a good, accurate technique for measuring C_p and Λ simultaneously. It has been shown that careful fits and corrections for light scattering are needed in order to obtain reliable results. The results obtained are in good agreement with the prediction of fluctuation calculations carried out within the framework of local mean-field theories. No deviations from these theories were found even very close to the clearing temperature. The exponent of C_p found here is very close to the Ornstein-Zernike value and agrees well with the correlation length obtained in the light-scattering experiment. Only partial agreement was found with the density measurements, which themselves happen to disagree with each other.

ACKNOWLEDGMENTS

It is a pleasure to thank Dr. E. Courtens for suggesting this problem, for many fruitful discussions, and for help in revising the manuscript. The author would also like to thank Dr. R. McFarlane for setting up the refractive-index system, T. Bischofberger for useful comments, and H. Amrein for technical assistance. The hospitality of everyone in the IBM laboratory during my stay there is gratefully acknowledged.

[1] J. Mayer, T. Waluga, and J. A. Janik, Phys. Lett. 41A, 102 (1972).
[2] R. Vilanove, E. Guyon, C. Mitescu, and P. Pieranski, J. Phys. (Paris) 35, 153 (1974).
[3] J. P. Gordon, R. C. Leite, R. S. Moore, S. P. S. Porto, and J. R. Whinnery, J. Appl. Phys. 36, 3 (1965).
[4] R. C. Leite, R. S. Moore, and J. R. Whinnery, Appl. Phys. Lett. 5, 141 (1964).
[5] P. Calmettes and C. Laj, J. Phys. (Paris) C 1, 125 (1972).
[6] M. Giglio and A. Vendramini, Appl. Phys. Lett. 25, 555 (1974).
[7] M. Giglio and A. Vendramini, Phys. Rev. Lett. 34, 561 (1975).
[8] M. Born, and E. Wolf, *Principles of Optics* (Pergamon, London, 1965), p. 306.
[9] D. Pohl (private communication).
[10] I. Haller, H. A. Huggins, and M. J. Freiser, Mol. Cryst. Liq. Cryst. 16, 53 (1972).
[11] M. J. Press and A. S. Arrott, Phys. Rev. A 8, 1459 (1973).
[12] R. Chang, Solid State Commun. 14, 403 (1974).
[13] E. Gulari and B. Chu, J. Chem. Phys. 62, 795 (1975).
[14] Reference 8, p. 123.
[15] M. Tournarie, J. Phys. (Paris) 30, 737 (1969).
[16] V. S. V. Rajan and J. J. C. Picot, Mater. Res. Bull. 9, 311 (1974).
[17] H. Imura and K. Okano, Chem. Phys. Lett. 17, 111 (1972).
[18] M. Arnold, Z. Phys. Chem. 226, 146 (1964).
[19] T. Shinoda, Y. Maeda, and M. Enokido, J. Chem. Thermodyn. 6, 921 (1974).
[20] B. Chu, C. S. Bak, and F. L. Lin, Phys. Rev. Lett. 28, 1111 (1972).
[21] T. W. Stinson and J. D. Litster, Phys. Rev. Lett. 30, 688 (1973).
[22] T. W. Stinson and J. D. Litster, Phys. Rev. Lett. 25, 503 (1970).

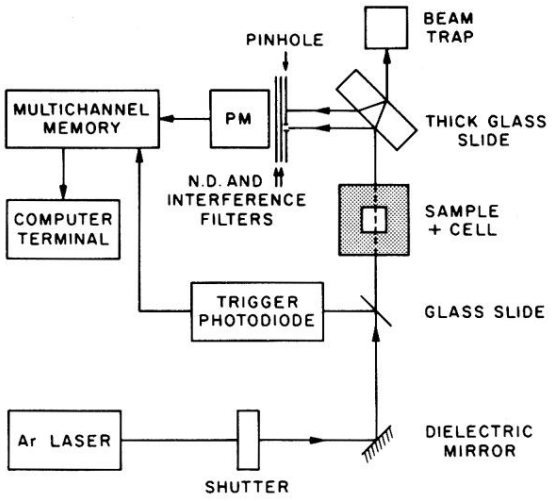

FIG. 1. Schematic diagram of the experimental system.